

Long Gamma-Ray Bursts and Their Host Galaxies at High Redshift

A. Lapi^{1,2}, N. Kawakatu^{3,2}, Z. Bosnjak^{4,2}, A. Celotti^{2,5}, A. Bressan^{6,2,7}, G.L. Granato⁶ and L. Danese²

¹Dip. Fisica, Univ. ‘Tor Vergata’, Via Ricerca Scientifica 1, 00133 Roma, Italy

²SISSA/ISAS, Via Beirut 2-4, 34014 Trieste, Italy

³National Astronomical Observatory of Japan, Mitaka, Tokyo 181-8588, Japan

⁴Institut d’Astrophysique de Paris, bd Arago 98bis, 75014 Paris, France

⁵INFN-Sez. di Trieste, Via Valerio 2, 34100 Trieste, Italy

⁶INAF-Osservatorio Astronomico di Padova, Vicolo dell’Osservatorio 5, 35122 Padova, Italy

⁷INAOE, Luis Enrique Erro 1, 72840 Tonantzintla, Puebla, Mexico

21 June 2024

ABSTRACT

Motivated by the recent observational and theoretical evidence that long Gamma-Ray Bursts (GRBs) are likely associated with low metallicity, rapidly rotating massive stars, we examine the cosmological star formation rate (SFR) below a critical metallicity $Z_{\text{crit}} \sim Z_{\odot}/10 - Z_{\odot}/5$, to estimate the event rate of high-redshift long GRB progenitors. To this purpose, we exploit a galaxy formation scenario already successfully tested on a wealth of observational data on (proto)spheroids, Lyman break galaxies, Ly α emitters, submm galaxies, quasars, and local early-type galaxies. We find that the predicted rate of long GRBs amounts to about 300 events $\text{yr}^{-1} \text{sr}^{-1}$, of which about 30 per cent occur at $z \gtrsim 6$. Correspondingly, the GRB number counts well agree with the bright *SWIFT* data, without the need for an intrinsic luminosity evolution. Moreover, the above framework enables us to predict properties of the GRB host galaxies. Most GRBs are associated with low mass galaxy halos $M_{\text{H}} \lesssim 10^{11} M_{\odot}$, and effectively trace the formation of small galaxies in such halos. The hosts are young, with age smaller than 5×10^7 yr, gas rich, but poorly extinguished ($A_V \lesssim 0.1$) because of their chemical immaturity; this also implies high specific SFR and quite extreme α -enhancement. Only the minority of hosts residing in large halos with $M_{\text{H}} \gtrsim 10^{12} M_{\odot}$ have larger extinction ($A_V \sim 0.7 - 1$), SFRs exceeding $100 M_{\odot} \text{yr}^{-1}$ and can be detected at submm wavelengths. Most of the hosts have UV magnitudes in the range $-20 \lesssim M_{1350} \lesssim -16$, and Ly α luminosity in the range $2 \times 10^{40} \lesssim L_{\text{Ly}\alpha} \lesssim 2 \times 10^{42} \text{erg s}^{-1}$. GRB hosts are thus tracing the faint end of the luminosity function of Lyman break galaxies and Ly α emitters. Finally, our results imply that the population of ‘dark’ GRBs occur mostly in faint hosts at high redshift, rather than in dusty hosts at low redshift.

Key words: Gamma-ray bursts, cosmic star formation, galaxies:evolution, galaxy:formation.

1 INTRODUCTION

The spectroscopic detection of the energetic supernova SN 2003dh coincident with GRB 030329 (Hjorth et al. 2003; Stanek et al. 2003) has firmly established that - at least some - long GRBs accompany the core collapse of massive stars, as it was first suggested by the spatial and temporal coincidence of GRB 980425 and SN 1998bw (Galama et al. 1998). Such spectroscopic signatures of supernovae (SNaE) associated with GRBs have been detected in a handful of cases during the last years, e.g. GRB 031203/SN 2003lw (Malesani et al. 2004), GRB 021211/SN 2002lt (Della Valle et al. 2003), GRB 050525A/SN 2005nc (Della Valle et al. 2006), and the recent case of GRB 060218/SN 2006aj (Campana et al. 2006, Modjaz et al. 2006). The possibility that core-collapse SNaE are progenitors of GRBs has been further supported by the detection of

re-brightening in the late-time afterglow light curves, interpreted as a contribution of accompanying SNaE (Bloom et al. 1999, Zeh et al. 2004, Castro-Tirado & Gorosabel 1999) and the localizations of afterglows in star forming regions (e.g. Djorgovski et al. 2001, Bloom et al. 2002, Fynbo et al. 2000, Fruchter et al. 1999, Holland & Hjorth 1999).

Indeed, the currently mostly favored scenario for the origin of long GRBs involves the collapse of a massive Wolf-Rayet star endowed with rotation (Woosley 1993, MacFadyen & Woosley 1999, Woosley & Heger 2004). Recently, Yoon & Langer (2005) considered the evolution of massive, magnetized stars where rapid rotation induces an almost chemically homogeneous evolution, and found that the requirements of this collapsar model are satisfied if the metallicity is sufficiently small, namely less than $0.1 Z_{\odot}$ (see

Woosley & Heger 2006; Yoon et al. 2006). This is broadly consistent with the estimates of metallicities of long GRB hosts, which yielded preferentially subsolar - down to $10^{-2} Z_{\odot}$ - values (e.g. Gorosabel et al. 2005; Chen et al. 2005; Starling et al. 2005).

Clearly this scenario has key implications not only on the physics of the event and on the evolution of massive stars at low metallicities, but also on the event rate and redshift distribution of long GRBs compared with that of SNaE. The cosmological consequences of a metallicity threshold can be explored by considering an average cosmic metallicity evolution, as in the work by Langer & Norman (2006). In the present paper we instead explore the effects of a metallicity threshold following the star formation and chemical evolution of individual galaxies.

In order to derive the rates of progenitors and the characteristics of their host galaxies at high redshift, the star formation history and the chemical evolution for a large range of galaxy mass and virialization redshift must be computed. Baryon condensation in cold gas, stars and in a central massive black hole (BH) within galaxy Dark Matter (DM) halos is a quite complex outcome of a number of physical processes (including shock waves, radiative and shock heating, viscosity, radiative cooling; star formation, BH accretion, gas inflow and outflow) largely affecting each other (see Granato et al. 2001, 2004; Croton et al. 2006; De Lucia et al. 2006). When treating these processes within a self-consistent cosmological framework of galaxy formation, most of the complexity is related to the different scales involved.

For the sake of definiteness, here we adopt as a reference the galaxy formation scenario developed by Granato et al. (2004), which consistently accounts for the coevolution of spheroidal galaxies and their nuclear activity and intrinsically follows in time the gas content, star formation rate (SFR) and metallicity evolution for each galaxy mass. This enables us to investigate in detail the effect of a metallicity threshold on the properties not only of the GRB population, but also of their host galaxies.

The outline of this paper is the following. In § 2 we briefly review the conceptual issues of the adopted galaxy formation scenario and explain how the GRB progenitor rate has been estimated. Our results are presented in § 3. In § 4 we discuss our findings, by comparing them with observational results and with previous studies. In § 5 we summarize our conclusions. Throughout the paper a flat cosmological model with matter density parameter $\Omega_M = 0.27$ and Hubble constant $H_0 = 72 \text{ km s}^{-1} \text{ Mpc}^{-1}$ is adopted.

2 MODELLING

2.1 Overview of the galaxy formation scenario

Long GRBs at high redshift ($z \gtrsim 1$) have progenitors which formed at least 8 Gyr ago. Their coeval stellar populations are as old as the populations of spheroidal galaxies and spiral bulges and older than the populations in present galaxy discs (see Renzini 2006); thus high redshift long GRBs trace the formation history of the oldest stellar populations. Low redshift GRBs conversely trace the star formation in small mass irregular/interacting galaxies with low SFR (Fruchter et al. 2006; Wainwright et al. 2007). Since we focus on high- z GRBs, in the following we will neglect the contribution of star formation in discs of present-day spiral galaxies.

We exploit the physical model elaborated by Granato et al. (2001, 2004), which follows the evolution of baryons within protogalactic spheroids taking into account the effects of the energy fed back to the intra-galactic gas by SN explosions and by accretion onto the nuclear supermassive BH (see also De Lucia et al.

2006; Croton et al. 2006). The model envisages that during or soon after the formation of the host DM halo, the baryons falling into the newly created potential well are shock-heated to the virial temperature. The hot gas is (moderately) clumpy and cools fast especially in the denser central regions, yielding a strong burst of star formation. Star formation also promotes the storage of the cooled gas into a reservoir around the central seed BH, eventually leading to accretion onto it (see Kawakatu & Umemura 2002). The ensuing SN explosions and the nuclear activity feed energy back to the baryons, and regulate the ongoing SFR and BH growth. These mutual energy feedbacks actually *reverse* the formation sequence of the baryonic component of galaxies compared to that of DM halos: the star formation and the buildup of central BHs are completed more rapidly in the more massive haloes, thus accounting for the phenomenon now commonly referred to as *downsizing* (e.g. Cowie et al. 1996; Kodama et al. 2004; Glazebrook et al. 2004).

In Appendix A we present a simplified version of basic equations of the model, which allow to derive analytical solutions for the time evolution of SFR, mass in stars and metallicity, the quantities relevant to this work. These analytical functions are very good approximations of the more complex system of equations numerically solved in Granato et al. (2004; see for details Lapi et al. 2006 and Mao et al. 2007). Because of their fundamental character, these equations catch the basic aspects of the physical processes ruling star formation in protogalaxies at high redshift. The adopted Initial Mass Function (IMF) is a double power-law with slope 1.25 from $120 M_{\odot}$ to $1 M_{\odot}$ and 0.4 from $1 M_{\odot}$ down to $0.1 M_{\odot}$ (Romano et al. 2002), which is quite similar to that proposed by Chabrier (2005).

In Fig. 1 we present the results for DM halos virialized at $z = 6$ and endowed with mass ranging from 10^{10} to $10^{13} M_{\odot}$. For masses $M_H \gtrsim 10^{12} M_{\odot}$ the SFR increases almost linearly with galaxy age in the initial stages, and then it is suddenly halted by the energy feedback from the quasar after a few 10^8 yr. On the contrary, for $M_H \lesssim 10^{12} M_{\odot}$ it is first almost constant and then slowly declines due to gas exhaustion. In fact, for small masses the effect of SNaE feedback regulates the star formation, while the BH is rather small there and the SFR can proceed for a much longer time (see Eq. [16] in Shankar et al. 2006).

The mass cycled through stars at any time is easily obtained by integrating the SFR (see Fig. 1). Note that the quantities plotted in Fig. 1 refer to redshift $z = 6$; however, both SFR and mass in stars scale approximately as $(1+z)^{3/2}$ for a given halo mass.

From the figure it is apparent that the chemical enrichment of the cold gas component is very rapid; e.g. with the adopted IMF the gas attains 1/100 and 1/10 the solar abundance in about 1.2×10^7 and 5×10^7 yr respectively, almost independently of the halo mass and redshift. A Salpeter IMF yields timescales about twice as long. This rapid enrichment is due to the fast evolution and formation timescales (t_* , see Appendix A) for the massive stars (greater than $10 M_{\odot}$) relative to the timescale for the infall of the diffuse medium with primordial composition, which dilutes the metallicity of the cold star-forming gas. This behavior shows that a possible change of the IMF at metallicity lower than a threshold around $3 - 5 \times 10^{-4} Z_{\odot}$ (see Bromm et al. 2001; Schneider et al. 2006) is not critical for the issue related to long GRBs. In other words, if long GRBs are associated with low metallicity environments, the quick enrichment implies that the most relevant epoch for GRB progenitors comes soon after halo virialization.

This galaxy formation model neglects spatial resolution and assumes instantaneous mixing, i.e. it averages both SFR and chemical composition over the entire mass of cold gas. We stress that the

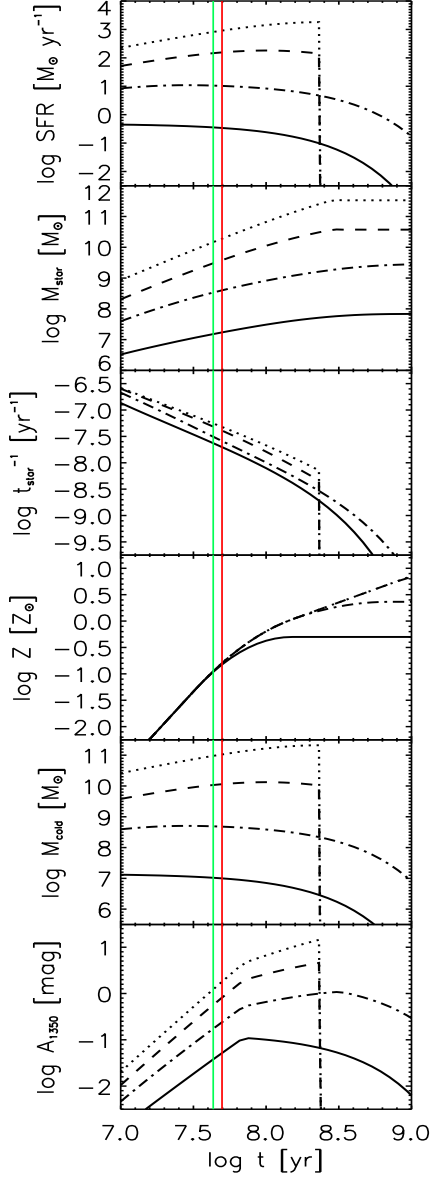


Figure 1. SFR, stellar mass, specific SFR, average cold gas metallicity, cold gas mass, and extinction at 1350 Å (from top to bottom) as a function of the galactic age for halos of masses $10^{10} M_{\odot}$ (solid lines), $10^{11} M_{\odot}$ (dotted lines), $10^{12} M_{\odot}$ (dashed lines), $10^{13} M_{\odot}$ (dotted lines), virialized at redshift $z = 6$. The vertical lines mark the epoch when the cold gas metallicity attains the critical thresholds $Z_{\odot}/10$ (green) and $Z_{\odot}/5$ (red).

cold gas is only a small fraction of the overall baryons associated with the galaxy halo (cf. Appendix A), and thus the averaging concerns the mass/volume of the protogalaxy wherein star formation is occurring and not the overall DM halo mass/volume. On the other hand, metallicity gradients have been observed in local spheroidal galaxies, $\Delta[Z/H]/\Delta \log r \approx -0.25$ (e.g. Annibali et al. 2007, Sanchez-Blancuez et al. 2007). This implies variations of about a factor two in metal abundance within a radius enclosing most of the galaxy mass. As we shall see such a factor is not crucial to the conclusions of this paper.

The model here adopted has the very valuable asset that successfully fits a wealth of observational data and constraints

regarding protospheroids, Lyman break galaxies and Ly α emitters, submm-selected galaxies, quasars, EROS and local early-type galaxies; for a detailed comparison with the observational data, we defer the interested reader to the papers by Granato et al. (2001, 2004, 2006), Cirasuolo et al. (2005), Silva et al. (2005), Lapi et al. (2006, in particular their Table 2), Mao et al. (2007); furthermore, clustering properties of submm galaxies have been extensively discussed in the context of our model by Negrello et al. (2007).

2.2 Estimate of long GRB progenitor rates

The key ingredients provided by the galaxy formation model related to this work are the SFR $\dot{M}_{\star}(t)$ and the average gas metallicity $Z(t)$ as a function of the age t for an individual galaxy within a given halo mass M_H virialized at redshift z (see Appendix A for handy approximations). Notice that Z refers to the average metallicity of the gaseous component from which new stars form.

The cosmic SFR per unit volume at redshift z contributed by objects with average gas metallicity $Z < Z_{\text{crit}}$ is thus given by

$$SFR(z)_{Z < Z_{\text{crit}}} = \int d\dot{M}_{\star} dM_H \frac{d^2 N_{\text{ST}}}{dM_H dt_z} \frac{d}{d \ln \dot{M}_{\star}} \mathcal{T}_{Z < Z_{\text{crit}}}^{\dot{M}_{\star}} \quad (1)$$

where $d^2 N_{\text{ST}}/dM_H dt_z$ are the formation rates of DM halos at cosmic time t_z computed using the Sheth & Tormen (1999) mass function, and $\mathcal{T}_{Z < Z_{\text{crit}}}^{\dot{M}_{\star}}$ is the time the galaxy spends at SFR higher than \dot{M}_{\star} and metallicity lower than Z_{crit} .

It is plausible that the core-collapse, believed to give rise to the formation of a BH and a GRB event, is related to the final phases of the evolution of stars with masses greater than $12 M_{\odot}$ and with rapidly rotating cores (Yoon & Langer 2005; Woosley & Heger 2006; Yoon et al. 2006). From a theoretical point of view a major issue in this respect is the large mass loss, that would entail also large angular momentum loss. This problem is possibly alleviated in stars of metallicity below a critical threshold lower than $1/5 - 1/3 Z_{\odot}$ and high initial spin rate (Woosley & Heger 2006; Yoon et al. 2006). Though observations are still scanty in supporting this expectation, we will consider low metallicity and high rotation velocity as necessary and sufficient conditions for a massive star to be considered as a GRB progenitor.

The GRB progenitor rate will thus be based on the above preliminary theoretical estimates which suggest that the expected fraction of GRB progenitors with respect to the number of massive stars ($8 M_{\odot} \lesssim m_{\star} \lesssim 100 M_{\odot}$) is $f_{\text{prog}} \gtrsim 2 - 3$ per cent for metallicity $Z_{\text{crit}} \lesssim Z_{\odot}/5$ (see Woosley & Heger 2006; Yoon et al. 2006).

The absolute GRB progenitors rate per unit volume can be then expressed as

$$\mathcal{R}_{\text{prog}}(z) = f_{\text{prog}} n_{\text{SN}} SFR(z)_{Z < Z_{\text{crit}}}, \quad (2)$$

where $n_{\text{SN}} \equiv \int_8^{100} \phi(m_{\star}) dm_{\star} / \int_{0.1}^{100} m_{\star} \phi(m_{\star}) dm_{\star}$ is the number of massive stars ending in SNaE per unit mass of formed stars; for the adopted IMF $n_{\text{SN}} \approx 1.4 \times 10^{-2} M_{\odot}^{-1}$ (it halves for a Salpeter IMF). Thus assuming $f_{\text{prog}} \approx 0.02$, the number of GRB progenitors per unit mass of formed stars amounts to about $3.6 \times 10^{-4} M_{\odot}^{-1}$ for $Z_{\text{crit}} \lesssim Z_{\odot}/5$.

2.3 Long GRB number counts

The number of GRBs at redshift greater than z is

$$\mathcal{R}_{\text{GRB}}^{\text{obs}}(> z) \approx f_{\text{beam}} \int_z^{\infty} dz' \frac{\mathcal{R}_{\text{prog}}(z')}{1+z'} \frac{dV}{dz'}, \quad (3)$$

where V is the cosmological volume per unit solid angle and the factor $(1+z)^{-1}$ accounts for time dilation effects due to redshift. Moreover, recall that GRBs are believed to be anisotropic phenomena owed to the flow collimation and/or relativistic beaming effects. Thus only a fraction f_{beam} of the estimated progenitors prompt emission would point toward us within an opening angle 2θ and could then be observed as a GRB. For the events for which a (jet) opening angle have been estimated¹ assuming that an afterglow light curve break owed to a jetted structure with a half angle θ (Ghirlanda et al. 2007), the median value $\theta \approx 6$ deg has been inferred (see also Guetta et al 2005); correspondingly, $f_{\text{beam}} \approx 5.5 \times 10^{-3} (\theta/6 \text{ deg})^2$. The expected number of long GRBs per unit mass of formed stars within metal poor environments ($Z \lesssim Z_{\text{crit}}$) is thus $k \approx 1.5 \times 10^{-6} (n_{\text{SN}}/1.4 \times 10^{-2}) (f_{\text{prog}}/0.02) (\theta/6 \text{ deg})^2 M_{\odot}^{-1}$.

The long GRB number counts at flux limit S_{lim} and redshift $> z$ is given as

$$\mathcal{R}_{\text{GRB}}^{\text{obs}}(> z)_{S>S_{\text{lim}}} \approx f_{\text{beam}} \int_z^\infty dz' \frac{\mathcal{R}_{\text{prog}}(z')}{1+z'} \frac{dV}{dz'} \int_{L_{\text{lim}}}^\infty P(L) dL; \quad (4)$$

in this expression $P(L)$ is the equivalent isotropic luminosity distribution (see § 3.2 for details), and L_{lim} is the luminosity corresponding to the limiting flux, given by

$$L_{\text{lim}}(z) = \frac{4\pi d_L^2(z)}{K(z)} S_{\text{lim}}, \quad (5)$$

in terms of the luminosity distance $d_L(z)$ and of the K -correction $K(z)$; note that the latter quantity depends on the GRB spectra, see § 3.2 for details.

3 RESULTS

3.1 Long GRB progenitor rates and redshift distribution

If progenitors of long GRBs are metal poor massive stars, the metal abundance Z of the cold gas wherein stars form is a crucial physical parameter. Fig. 2 shows the cosmological SFR for the overall galaxy population and for systems with $Z \lesssim Z_{\text{crit}} \approx 0.1$ and $0.2 Z_{\odot}$ as function of redshift. The model prediction can be fitted with the approximate formula

$$\log \left(\frac{\text{SFR}(z)_{Z < Z_{\text{crit}}}}{M_{\odot} \text{ yr}^{-1} \text{ Mpc}^{-3}} \right) = a + b(z - z_{\text{max}})^2, \quad (6)$$

where $a = -1.4 (-3.2)$, $b = -3.8 (-3.2) \times 10^{-2}$ and $z_{\text{max}} = 4.5 (6.5)$ for $Z_{\text{crit}} = 0 (Z_{\odot}/10)$.

The predicted overall SFR reproduces fairly well the extinction-corrected data at $2 \lesssim z \lesssim 6$, with reasonable correction for dust extinction. At $z \lesssim 1$ the observed SFR is underestimated due to the fact that intrinsically our model does not account for the contribution of star formation in discs of present spiral galaxies. On the other hand, only a minor fraction (less than 20 per cent) of long GRBs with redshift determination (though it is difficult to quantify the observational biases which certainly affect this percentage) are located at $z \lesssim 1$, while we are interested in the bulk of the (high redshift) GRB population (cf. § 2.1).

As expected the SFR in GRB hosts decreases with Z_{crit} , but the effect is differential with redshift. Since the timescale

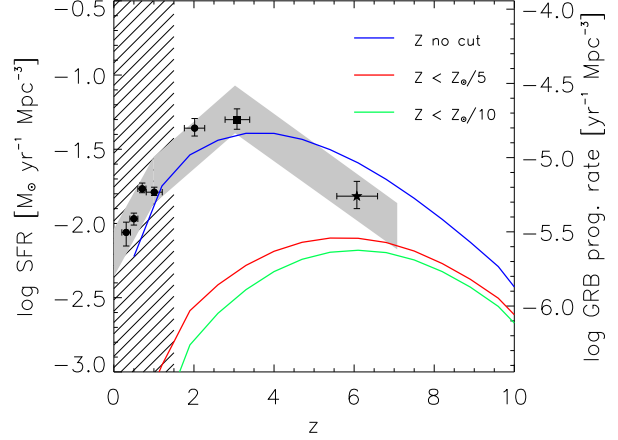


Figure 2. Cosmological SFR (left y-axis) and rate of long GRB progenitors (right y-axis) as a function of redshift, computed with no threshold on metallicity (blue line), and with thresholds at $Z_{\odot}/5$ (red line) and $Z_{\odot}/10$ (green line). Data are from Schiminovich et al. (2005; circles), Steidel et al. (1999; squares), and Bouwens et al. (2006; stars). The shaded area illustrates the uncertainties due to the extinction correction; the data have been rescaled down by a factor of about 2 to account for the adopted IMF (see text). In the hatched region the SFR is dominated by discs of present spiral galaxies, not treated in our model.

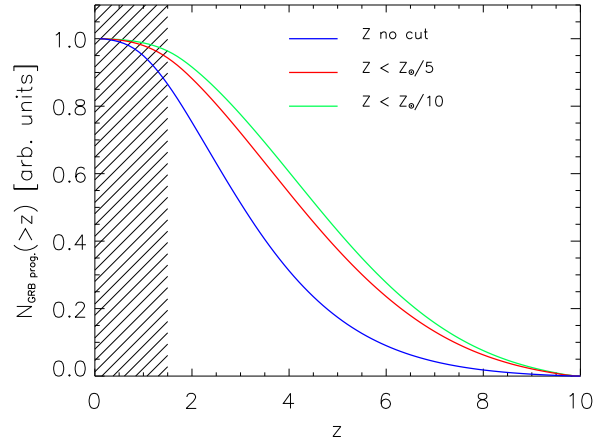


Figure 3. Normalized redshift distribution of GRB progenitors, computed with no threshold on metallicity (blue line), and with thresholds at $Z_{\odot}/5$ (red line) and $Z_{\odot}/10$ (green line).

$t_{\text{crit}} \lesssim 5 \times 10^7$ yr to reach the critical metallicity threshold is almost independent of mass and redshift (cf. Fig. 1), its ratio to the cosmic time increases toward high z for all halos. The fraction of overall cosmic star formation occurring in metal poor protogalaxies raises with redshift, and so does the predicted rate of GRB progenitors. The net effect is that the expected redshift distribution of long GRB progenitors peaks to a redshift significantly higher than that of the cosmic SFR. As a consequence the higher the redshift, the more directly GRBs mirror the cosmic SFR. The fall off of star formation beyond $z \gtrsim 10$ in the galaxy formation model is a consequence of the effect of the SN feedback; at increasing z the decrease of star formation $\propto M_{\text{H}}^{1.5}$ is not balanced by the rise in the number of virialized halos.

¹ These estimates maybe clearly affected by selection effects, though not easy to quantify.

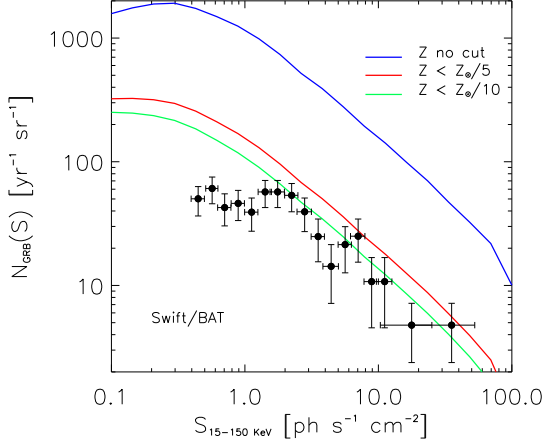


Figure 4. GRB counts in the 15 – 150 keV band, computed with no threshold on metallicity (blue line), and with thresholds at $Z_{\odot}/5$ (red line) and $Z_{\odot}/10$ (green line). Data (filled dots) are from the 2-yr *SWIFT* catalog.

The long GRB progenitor rate shown in Fig. 2 can be integrated over cosmic time to obtain the normalized redshift distribution reproduced Fig. 3. For the case $Z_{\text{crit}} = Z_{\odot}/10$, the fraction of progenitors is around 60 per cent at $z \gtrsim 4$ and around 30 per cent at $z \gtrsim 6$.

If the threshold Z_{crit} were to refer to stellar rather than ISM metallicity, the time within which GRB progenitors can be produced in any galaxy halo would be overestimated by a factor around 2. This would in turn double the duty cycle and, hence, the number of progenitors. The difference in the predictions worsens with higher Z_{crit} threshold, to the point where the threshold might never be reached in small galaxies, which then can host GRB progenitors over the whole Hubble time. Again the effect is differential with redshift, with a larger increase in the progenitor number at higher z .

3.2 Long GRB counts with *SWIFT*

In order to assess whether a scenario in which single metal poor, rotating massive stars are the GRB progenitors is tenable within the adopted galaxy model framework, we estimated the predicted long GRB counts which should have been detected by *SWIFT* (Gehrels et al. 2004).

As discussed in § 2.2 and § 2.3 we consider a number of observed GRBs per unit mass $k \approx 1.9 \times 10^{-6} M_{\odot}^{-1}$ and a metallicity threshold $Z_{\text{crit}} \approx 1/10 - 1/5 Z_{\odot}$.

In order to estimate the observable number of GRBs as function of limiting flux, we assume that the prompt GRB luminosity distribution can be characterized, independently of redshift, as

$$P(L) \propto L^{-\delta} e^{-L_c/L}, \quad (7)$$

with a low luminosity cutoff at $L_c = 3 \times 10^{51} \text{ erg s}^{-1}$, and slope $\delta = 2$. This parametrization is consistent with those constrained by Daigne et al. (2006) and Guetta et al. (2005). As for the spectrum, we adopted - as commonly done - a typical Band representation, with low and high energy slopes $\alpha = -1$ and $\beta = -2.25$, respectively. The peak energy is considered to follow a log-normal distribution (Preece et al. 2000) with mean $\log E_{\text{peak},0} = 2.74$ and dispersion $\sigma = 0.3$ dex (see Daigne et al. 2006). Although such spectral parameters have been estimated from bright *BATSE* GRBs

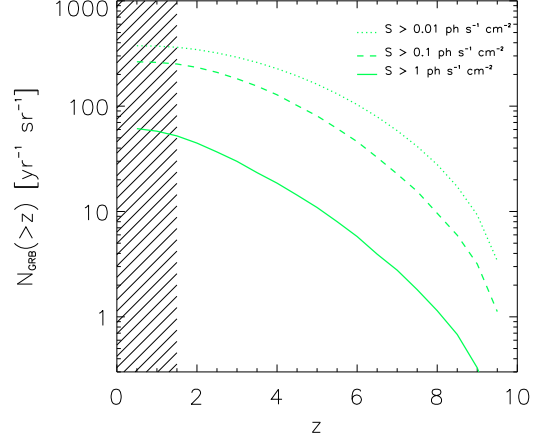


Figure 5. The redshift distribution of GRBs at the limiting flux [15-150 keV] of 0.01 (dotted line), 0.1 (dashed line), and $1 \text{ ph s}^{-1} \text{ cm}^{-2}$ (solid line), computed with a threshold on metallicity at $Z_{\odot}/10$.

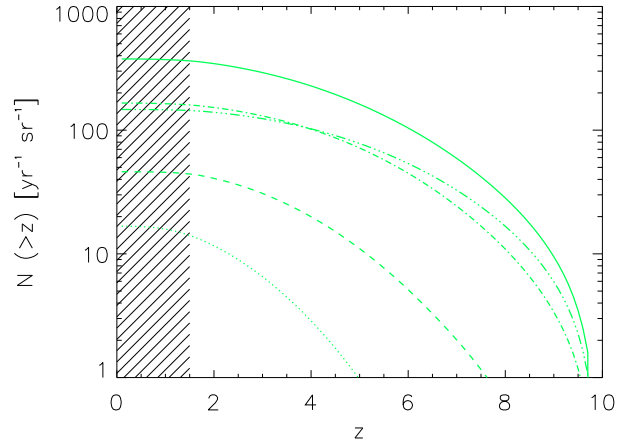


Figure 6. The redshift distribution of GRBs computed with a threshold on metallicity at $Z_{\odot}/10$ (solid line). The other curves illustrate the contributions from host galaxies with different halo masses: $10^9 - 10^{10} M_{\odot}$ (triple-dot-dashed line), $10^{10} - 10^{11} M_{\odot}$ (dot-dashed line), $10^{11} - 10^{12} M_{\odot}$ (dashed line), $10^{12} - 10^{13} M_{\odot}$ (dotted line).

(Preece et al. 2000), this provides the simplest hypothesis which - given the relatively small effect owed to the K -correction - appears adequate for the consistency check we intended to perform.

The predicted number counts are shown in Fig. 4 together with the actual *GRB SWIFT* counts. A meaningful comparison can only consider ‘bright’ *SWIFT* GRBs, namely above a photon flux of $1 \text{ ph s}^{-1} \text{ cm}^{-2}$, as below this level some degree of incompleteness is expected (Band 2006).

As it is apparent from Fig. 4 a reasonable agreement with the *SWIFT* counts can be obtained after the above assumptions. It should be pointed out that we did not perform any fitting optimization, but simply compared the counts predicted by the model with the data, under the simplified and commonly adopted assumptions on the luminosity and spectral energy GRB distributions outlined above.

A very interesting aspect concerns the fact that the counts can be reasonably reproduced without requiring any GRB prompt lu-

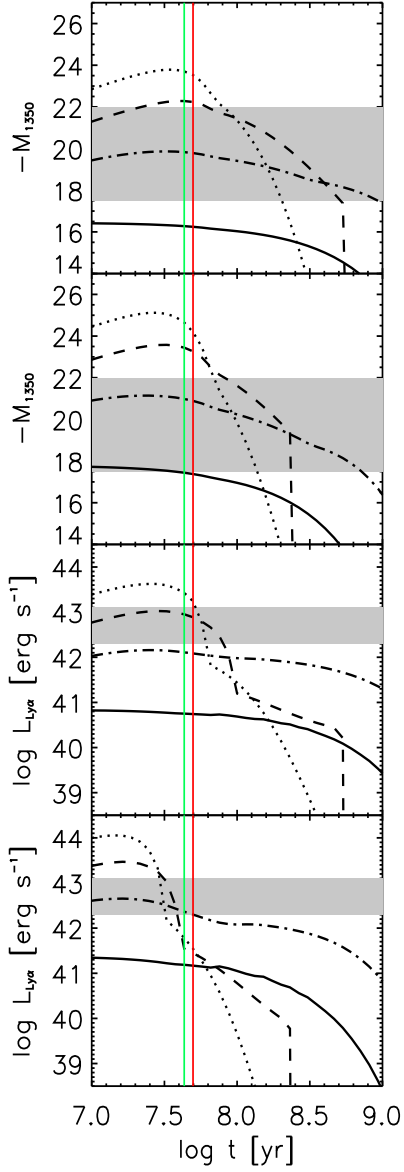


Figure 7. Extincted magnitude at 1350 Å and Ly α luminosity of the host galaxies of the GRB progenitors as a function of galactic age. Lines as in Fig. 1. The first and third panels refer to redshift 3, the second and forth ones to redshift 6. The *shaded* areas illustrate the ranges sampled in the observed luminosity functions.

minosity evolution (e.g. Daigne et al. 2006). This is a natural consequence of the fact that our redshift progenitor distribution intrinsically peaks at redshift higher than the cosmic star formation. Indeed, if we were to reproduce the number counts with no metallicity threshold, the number of GRBs per unit mass of formed stars (k) would have to be a factor about 10 lower, which would imply that the bulk of the progenitors would be located at lower redshift.

The predicted redshift distribution of GRB events for different flux limits is presented in Fig. 5. This shows that already at fluxes $S \gtrsim 1 \text{ ph s}^{-1} \text{ cm}^{-2}$ we expect that 10 per cent of GRBs occur at $z \gtrsim 6$. Of course such a fraction increases with decreasing limiting flux, reaching around 30 per cent for $S \gtrsim 10^{-2} \text{ ph s}^{-1} \text{ cm}^{-2}$; since this flux limit is below the present detectable level, the upper

curve of Fig. 5 represents the redshift distribution of all currently observable GRBs.

More specifically, the model predicts that in two years 13 GRBs at $z \gtrsim 6$ and flux limit $1 \text{ ph s}^{-1} \text{ cm}^{-2}$ should have been detected by *SWIFT*. So far only 1 GRB has robust redshift estimate at $z > 6$. On the other hand, while it is difficult to quantify the efficiency of the redshift determination, especially for very high redshift events, this could well be less than 10 per cent.

3.3 GRB host galaxies

The exploited galaxy formation model also enables us to directly predict the properties of the GRB host galaxies (SFR, magnitude, stellar mass, average metallicity, extinction) as function of the halo mass and age as well as the luminosity function (LF) and the corresponding SFR distribution of the overall population.

As discussed in § 2.1, during the evolution of individual galaxies, the metallicity of the star-forming gas attains the threshold $Z_{\text{crit}} = 0.1 - 0.2 Z_{\odot}$ quite rapidly, within $t_{\text{crit}} \approx 5 \times 10^7$, and this timescale is basically independent of the host halo mass.

Interestingly, since this is much shorter than the halo virialization timescale, $t_{\text{crit}} \ll t_{\text{H}}$, the GRB rates for fixed halo mass directly trace the cosmic rate of halo virialization. As a consequence, the GRB hosts mostly reside within galaxy halos in the mass range $10^9 \lesssim M_{\text{H}} \lesssim 10^{11} M_{\odot}$, and only at $z \lesssim 4$ the fraction of hosts in massive halos $M_{\text{H}} \gtrsim 10^{11} M_{\odot}$ exceeds 10 per cent. The relative number of GRBs for different halo masses as function of redshift is shown in Fig. 6.

The predicted evolution of the SFR and stellar mass as functions of galactic age and halo mass are reported in Fig. 1. For halo masses in the range $10^{10} - 10^{13} M_{\odot}$ and virialized at redshift $z \approx 6$ the expected SFR spans $0.3 - 10^3 M_{\odot} \text{ yr}^{-1}$, and the corresponding stellar masses cover the interval $10^7 \lesssim M_{\star} \lesssim 2 \times 10^{10} M_{\odot}$, with both quantities scaling as $(1+z)^{3/2}$ at a given halo mass. The shortness of t_{crit} yields high specific SFRs, $\dot{M}_{\star}/M_{\star} \gtrsim 2 \times 10^{-8}$, almost independently of the virialization redshift.

Now we turn to consider more directly observable properties of GRB hosts, such as the average ultraviolet extinction A_{1350} and the corresponding extincted magnitude M_{1350} at 1350 Å, again as function of galactic age. We recall that $M_{1350} \approx -18.6 - 2.5 \log(\dot{M}_{\star}/M_{\odot} \text{ yr}^{-1}) + A_{1350}$ (see Appendix A). Fig. 1 reports A_{1350} , which scales with redshift as $(1+z)^{3/5}$, for various halo masses virialized at redshift $z = 6$. A key prediction of the model is apparent, namely that most GRB hosts are poorly extinguished systems. Since the less massive hosts ($M_{\text{H}} \lesssim 10^{11} M_{\odot}$) largely outnumber the most massive ones, the typical A_{1350} ranges between 0.01 – 0.3 mag, corresponding to $A_{\text{V}} \lesssim 0.1$. Larger dust extinction is predicted only for more massive hosts $M_{\text{H}} > 10^{11} M_{\odot}$, which exceed a few per cent of the total GRB hosts only at $z \lesssim 6$ (cf. Fig. 1).

The AB absolute magnitude at 1350 Å, M_{1350} , is reported in Fig. 7 for various halo masses and redshifts $z = 3$ and $z = 6$. The shaded area indicates the absolute magnitude range where the UV high- z LF is currently well sampled. It is clear that the UV luminosity is practically not affected by dust, since the predicted extinction is low for galaxy ages less than t_{crit} .

Fig. 7 also shows the age dependence of the expected Ly α luminosity at fixed halo mass. At variance with respect to the behavior of the UV magnitude, the Ly α luminosity of hosts in larger halos is already declining for ages less than t_{crit} at $z \gtrsim 6$, since Ly α

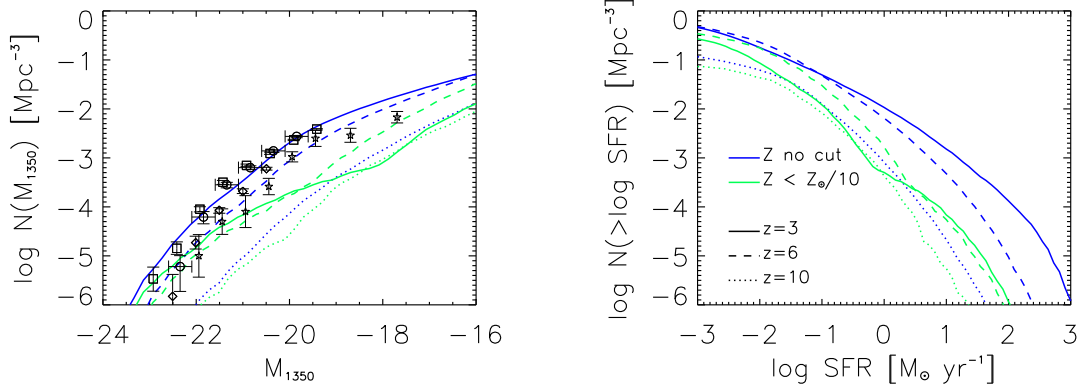


Figure 8. The comoving number density of galaxies as a function of UV magnitude at 1350 Å M_{1350} (left) and of SFR (right). In both panels *solid*, *dashed* and *dotted* lines refer to redshifts $z = 3, 6$, and 10 , respectively. The sets of *blue* and *green* curves refer to no metallicity threshold and $Z_{\text{crit}} = Z_{\odot}/10$. The data points reported in the left hand panel are from Steidel et al. (2001; *circles*) and Yoshida et al. (2006; *squares*) at $z \sim 3 - 4$, Yoshida et al. (2006; *diamonds*) at $z \sim 4 - 5$, and Bouwens et al. (2006; *stars*) at $z \sim 5 - 7$.

emission is sensitive not only to dust but also to neutral hydrogen absorption.

Anyhow we expect a strict correlation between GRB hosts and Lyman Break Galaxies (LBG) and Ly α emitters (LAE). As the galaxy model here adopted reproduces the high-redshift UV LF of LBGs and LAEs (see Mao et al. 2007), it is meaningful to estimate the UV LF expected for GRB hosts, namely by imposing the condition $Z \lesssim Z_{\text{crit}} \approx 0.1 Z_{\odot}$. The result is shown in Fig. 8. In general the conditional UV LF depends on the ratio between t_{crit} and the time during which the host is brighter than a fixed absolute magnitude. As expected, the metallicity cut depresses the UV luminosity distribution, but this depression is minimal at the faint and bright ends, and maximum at intermediate values, as expected from the effects of the cut on M_{1350} in individual systems.

In particular, the time spent by galaxies in large halos as LBGs - before turning into strongly submm emitting galaxies because of dust attenuation - is short and comparable with t_{crit} . At the faint end the luminosity of small hosts can fall below a fixed magnitude in a relatively short time, as shown in Fig. 8 for hosts in halos with $M_{\text{H}} \approx 10^{10} M_{\odot}$. It is also apparent that intermediate mass halos and the corresponding intermediate UV luminosity objects are significantly more affected by the condition on metallicity. Obviously at high redshift, e.g. $z \approx 10$, the cut reduces the visibility timescale only by a small fraction.

We can conclude that GRB hosts should well reproduce the LBG LF at its faint and bright ends. Similar conclusions hold for LAE LF.

The shortness of $t_{\text{crit}} \approx 50$ Myr implies that the hosts must exhibit quite large $[\alpha/\text{Fe}]$ enhancement. In fact, the cumulative fraction of SNIa explosions after an instantaneous burst of star formation (1 at 12 Gyr) is negligibly small for 50 Myr (corresponding to the lifetime of a $7 M_{\odot}$ star), for a wide class of progenitor models, i.e. Single Degenerates (SD), and Double Degenerates (DD) exploders (Greggio 2005). At 0.1 Gyr it reaches 10 per cent in the most favorable case of close DD scheme. Furthermore, the typical timescales required to significantly decrease the $[\alpha/\text{Fe}]$ ratio from its initial value produced by a single generation of massive stars (approximately 0.4 – 0.6 depending on metallicity, IMF and stellar yields, Gibson et al. 2003), is 0.3, 1 and 3 Gyr, for close DD, SD and WIDE DD progenitors, respectively. Thus while in the

most massive ellipticals the duration of the burst of star formation (around 0.3 Gyr) may be enough for a mild pollution by Fe-peak elements (depending on the assumed scenario for SNIa progenitors), the lower timescale required to reach the critical metallicity implies that GRB hosts should display the original pattern of heavy elements produced by massive star chemical evolution. Notice that the subsequent history of star formation decreases the initial α -enhancement more in smaller than in larger objects (see Fig. 1). We conclude that at high redshift, GRB hosts (and the similarly young LAEs) exhibit the highest values of α -enhancement, even higher than those of high- z quasar hosts and of their descendents, the massive elliptical galaxies.

Finally, we can also estimate the distribution of intrinsic SFRs. It is worth stressing that generally the hosts with SFRs exceeding a few $\times 10^2 M_{\odot} \text{ yr}^{-1}$ are significantly less than the overall galaxy population. This suppression reflects not only the steep halo mass function, but also the short duty cycle of GRB hosts following the rapid metal enrichment in the initial stages of star formation. And again the effect gets more pronounced at decreasing z due to the increased fraction of observable hosts which are below threshold. On the other hand, the model allows for the existence of GRB hosts with SFRs exceeding a few $\times 10^2 M_{\odot} \text{ yr}^{-1}$ within halos endowed with $M_{\text{H}} \gtrsim 10^{12} M_{\odot}$: as shown in Fig. 1 and Fig. 8, the fraction of these hosts should amount to a few per cent of the total. Nevertheless they should not have formed a large amount of stars $M_{\star} \lesssim 10^{10} M_{\odot}$, exhibit specific SFR $\dot{M}_{\star}/M_{\star} \gtrsim 10^{-8} \text{ yr}^{-1}$ and should be rather extinguished by dust (see Fig. 1).

4 DISCUSSION

The adopted galaxy formation scenario coupled with the metal poor collapsar model suggested by stellar evolution have been exploited to infer the above results, which include GRB counts and redshift distribution and the complete description of the relevant properties of their hosts, such as SFR, mass in stars, chemical evolution in the cold star forming gas and in the stellar component within individual galaxy halos, with specified mass and formation redshift. In this § 4 these results are discussed in the light of presently available observations and they are compared to previous studies.

4.1 GRB progenitor rates and GRB counts

The imposed metallicity threshold affects the GRB progenitor redshift distribution. Instead of peaking at around $z \approx 3$ as in the case without metallicity constrain, the threshold $Z_{\text{crit}} = Z_{\odot}/10$ yields a broad peak at $z \approx 6$ (Fig. 2). A significant fraction of progenitors are expected at high redshift: approximately 60 per cent at $z \gtrsim 4$ and approximately 30 per cent at $z \gtrsim 6$ (see Fig. 3). This behavior is shared by all models which associate GRBs with metal poor progenitors (e.g. Natarajan et al. 2005; Langer & Norman 2006; Salvaterra & Chincarini 2007).

In particular, our findings are similar to those inferred by Langer & Norman (2006), who explored the effect of a metallicity threshold in the environment of GRBs, by adopting a mass-stellar metallicity relation for galaxies and an average cosmic metallicity $[Z]$ dependence on redshift $d[Z]/dz \approx -0.15$ dex. This law, derived to reproduce the metallicity of stars in galaxies, has been extrapolated to the ISM. This extrapolation implies that at $z \gtrsim 7$ all cosmic star formation occurs in environments with $[Z] \lesssim 0.1 Z_{\odot}$, independently of the processes occurring in galaxy halos. As a result the corresponding rate of low metallicity SNaE peaks at $z \approx 6$. In our model the combination of cooling and feedback processes implies that at $z \approx 7$ the SFR in cold gas with $Z \lesssim 0.1 Z_{\odot}$ amounts to about 40 per cent of the cosmic one, due to the short timescale for gas enrichment. Therefore, despite of the quite different approach, the redshift distributions of GRB progenitors found by Langer & Norman (2006) and Yoon et al. (2006) are very similar to ours, since their assumed SFR for metal poor stars peaks at $z \approx 6$, similarly to our SFR in cold gas environment (see Fig. 2).

The combination of the galaxy formation scenario with the low metallicity collapsar hypothesis for GRB events leads to a good agreement of the predicted and observed (bright, $S \gtrsim 1 \text{ ph s}^{-1} \text{ cm}^{-2}$) *SWIFT* counts (see Fig. 4). This naturally follows - without any tuning - from the derived number of GRB progenitors, under quite simple and plausible assumptions on the GRB jet opening angle, prompt gamma-ray luminosity distribution and spectral shape, without requiring any luminosity evolution (see § 2.3 and § 3.2).

The corresponding redshift distribution (see Fig. 5) implies that at this bright limit the adopted model predicts about 6 GRBs per year, while only one GRB at $z \gtrsim 6$ has been identified in two years of *SWIFT* operation. As a matter of fact, only for about half of the *SWIFT* bursts an optical afterglow has been observed, and for only 30 per cent it has been possible to infer a redshift estimate. It is therefore quite reasonable to guess that this fraction could be about 10 per cent for bursts at $z \gtrsim 6$ (see Fiore et al. 2007).

Recently Salvaterra & Chincarini (2007) obtained a good formal fit to the *SWIFT* counts down to $S \approx 0.4 \text{ ph s}^{-1} \text{ cm}^{-2}$, adopting as free parameters the count normalization and the GRB LF (two further parameters). They considered the case of low metallicity environment by adopting a kinematical model and predict the occurrence of only 1 GRB yr^{-1} for the *SWIFT* bright flux limit ($1 \text{ ph s}^{-1} \text{ cm}^{-2}$). Their result imply a redshift determination efficiency for GRBs greater than 50 per cent.

It is worth noticing that reaching completeness down to $0.1 \text{ ph s}^{-1} \text{ cm}^{-2}$ would significantly increase the number of detected GRBs and in turn allow to explore the Universe during the recombination epoch, $z \gtrsim 8$, with good statistical significance. A further decrease in the flux limit to $0.01 \text{ ph s}^{-1} \text{ cm}^{-2}$, would instead only increase the GRB sample by a factor of 2; at this flux limit practically all GRBs would be detected (see Figs. 5 and 6).

In order to account for the trend of GRBs to be at substantial redshift Firmani et al. (2005) proposed that the GRB LF is

evolving. Daigne et al. (2005) tested the hypothesis of an increasing efficiency of GRB production by massive stars with increasing redshift. Detailed redshift distributions of GRBs will discriminate among these different possibilities.

We can conclude that the hypothesis that metal-poor, rapidly rotating massive stars are the GRB progenitors (Woosley & Heger; Yoon et al. 2006) is consistent with the observed *SWIFT* counts. Clearly determinations of GRB redshifts will be extremely informative on the progenitor and galaxy formation models.

We stress that the adopted galaxy formation scenario exploits quite a standard IMF, independent of the gas metallicity. As a matter of fact, we showed that the cold star forming gas is rapidly ($t \ll 10^7 \text{ yr}$) enriched to the possible threshold around $3 - 5 \times 10^{-4} Z_{\odot}$, below which the IMF might be strongly biased toward high mass stars (see Bromm et al. 2001; Schneider et al. 2006). Therefore the possible contribution of pop III stars with IMF strongly biased toward high masses is not considered here. However, Bromm & Loeb (2006) showed that at $z \approx 10$ the contribution of pop III to cosmic SFR could be of order of 1/10 of the overall SFR, becoming dominant at $z \gtrsim 15$; the GRB rate from pop III massive stars would grow correspondingly.

4.2 Properties of Long GRB Host Galaxies

Though the idea that GRBs are preferentially located in metal poor environments is attractive, nevertheless observational estimates of the metal content of host galaxies are still controversial. While most of the results suggest that at high- z GRB hosts exhibit metallicity $Z \lesssim 0.1 - 0.3 Z_{\odot}$ (Prochaska et al. 2007, Price et al. 2007), there are claims of higher metal content (see Savaglio et al. 2003).

Once a metal poor ($Z \sim 0.1 Z_{\odot}$) collapsar model is assumed, our galaxy formation scenario predicts that GRB hosts are very young, with age less than $5 \times 10^7 \text{ yr}$, independently of the halo mass. This young age directly mirrors the predicted short timescale, $t_{\text{crit}} \approx 5 \times 10^7 \text{ yr}$, of chemical enrichment of the cold gas, independently of mass. Such independence makes the GRB rate at high- z a good tracer of the virialization rate of relatively small galaxy halos, $M_{\text{H}} \lesssim \times 10^{11} M_{\odot}$ (see Fig. 6).

A definite prediction issuing from their youth is that GRB hosts should exhibit high $[\alpha/\text{Fe}]$ -enhancement, as their metal content directly reflects the chemical yields of core collapse SNaE. Indeed, in the most favorable scenario of close DD progenitors, type Ia SNaE may halve the $[\alpha/\text{Fe}]$ ratio produced by the generations of massive stars in a few 10^8 yr , somewhat longer than t_{crit} . Recent observations by Prochaska et al. (2007) suggest that α/Fe ratios are more than 3 times the solar value. Though differential depletion could be responsible for the result, the young age of the hosts is a much more palatable explanation.

The shortness of t_{crit} implies that star formation has not much proceeded, i.e. the model predicts high specific star formation $\dot{M}_{\star}/M_{\star} \gtrsim 2 \times 10^{-8} \text{ yr}^{-1}$. Notice that even the specific star formation is almost independent of halo mass. Specific SFRs at this high level have been claimed by several authors (Fruchter et al. 1999; Le Floch et al. 2003; Christensen et al. 2004; Savaglio et al. 2006; Michalowski et al. 2007). We caution that metal poor gas may be left over particularly in external regions of relatively old galaxies, hosting a burst of star formation even if most stars already formed and the gas was already metal enriched. However, we expect that relatively evolved hosts endowed with significant stellar mass are exceptions: GRB 020127 could be one of such cases (Berger et al. 2007). The vast majority of GRBs are hosted by small galaxies soon after their first stars shine.

Since the hosts are very young galaxies, our model predicts that they are gas rich objects with large column density N_{H} , once more independently of their galaxy halo mass. Observations confirm the tendency for GRB hosts to exhibit large N_{H} (Prochaska et al. 2007; Schady et al. 2007). At odd with these results, Tumlinson et al. (2007) set stringent upper limits on the molecular hydrogen (H_2) abundance, concluding that the fraction of molecular hydrogen H_2/HI is extremely low in the examined hosts. These authors also point out that the deficiency may be related to low dust abundance, H_2 formation being catalyzed on the surface of dust grains. An additional possibility is the destruction of H_2 by UV radiation. The model here proposed predicts that GRB hosts are dust poor and are pervaded by a intense UV radiation field; therefore they are expected to be quite poor in molecular hydrogen.

Concerning the UV emission, most of the hosts ($M_{\text{H}} \lesssim 10^{10} M_{\odot}$) should have UV magnitude at 1350\AA in the range $-20 \lesssim M_{1350} \lesssim -16$. The most luminous hosts are bright enough to be included in the already available LBG LF. Interestingly, Jakobsson et al. (2005) have shown that GRB hosts are tracing the faint end of the LBG LF at $z \approx 3$.

The predicted host $\text{Ly}\alpha$ luminosity should fall in the interval $2 \times 10^{40} \lesssim L_{\text{Ly}\alpha} \lesssim 2 \times 10^{42} \text{ erg s}^{-1}$, only marginally overlapping with the range explored by currently available $\text{Ly}\alpha$ LF (Fig. 7). Tanvir & Levan (2007) have shown that the UV rest frame luminosity distribution of $\text{Ly}\alpha$ selected galaxies and GRB hosts at $z \sim 3$ are quite similar. We notice that Mao et al. (2007) pointed out that LAE are expected to be younger, with lower stellar masses, more compact and associated with less massive halos than LBGs.

In summary, observations supports the model prediction that the GRB hosts trace the faint end of the LF of LBGs and LAEs.

A further issue concerns the amount of dust in GRB hosts. While most hosts have not been detected at mid-IR or submm wavelengths (e.g. Tanvir et al. 2004; Le Flocc'h et al 2006; Priddey et al. 2006) in a few cases submm and radio emission have been actually detected (Michalowski et al. 2007). How can the existence of these hosts be interpreted within the proposed scenario?

The model predicts that only GRBs hosted in large galactic halos $M_{\text{H}} \gtrsim 10^{12} M_{\odot}$ can have significant dust absorption. These also exhibit large SFR ($\dot{M}_{\star} \gtrsim 100 M_{\odot} \text{ yr}^{-1}$) and relatively small stellar mass ($M_{\star} \lesssim 10^{10} M_{\odot}$). These properties correspond to those inferred by Michalowski et al. (2007) for the submm and radio detected objects. The model also predicts that these systems should represent only 1/20 of all the GRB hosts at $z \approx 1 - 2$ and practically disappear at $z \gtrsim 5$.

We stress that the conclusions regarding the host properties refer to the average GRB population, and do not exclude the possibility that individual GRBs might reside in low metallicity local regions within their host (as might be the case for GRB 060206, Fynbo et al. 2006).

The above findings have been derived in the framework of a galaxy formation scenario, where a key role is played by the energy feedbacks provided by SNaE and quasars. However, the fast chemical enrichment leading to gas metallicity above $Z_{\text{crit}} \approx 0.1 Z_{\odot}$ takes place at early galactic times, before quasar feedback becomes effective. On the other hand, the stellar feedback is very relevant since it regulates the star formation activity even at early galactic times.

5 SUMMARY

We have explored the cosmological consequences of the assumption that metal poor and rapidly rotating single stars are the progenitors of most long GRBs. Our main conclusions are:

- The overall long GRB rate amounts to approximately $300 \text{ yr}^{-1} \text{ sr}^{-1}$. Bright *SWIFT* counts are reproduced by assuming a non-evolving prompt (gamma-ray) luminosity distribution.
- Above a flux limit of $1 \text{ ph s}^{-1} \text{ cm}^{-2}$ about 30 per cent of GRBs are predicted to be at $z \gtrsim 6$ and 10 per cent at $z \gtrsim 8$, amounting to approximately 13 for two years of *SWIFT* operation. Only one have been located above $z \gtrsim 6$ in two years: this would require a redshift determination efficiency around 10 per cent, to be compared with the 30 per cent efficiency for events at lower z .
- The host galaxies are very young, with age less than $5 \times 10^7 \text{ yr}$, gas rich (large column densities) but poorly extinguished systems ($A_{\text{V}} \lesssim 0.1$), because of their chemical immaturity. Only the few per cent of hosts associated with large halos ($M_{\text{H}} \gtrsim 10^{12} M_{\odot}$) have large extinction ($A_{\text{V}} \gtrsim 0.3$), high SFR ($\dot{M}_{\star} \gtrsim 100 M_{\odot} \text{ yr}^{-1}$) and can be detected at relatively bright submm flux levels. This result has implications for the origin of ‘dark’ GRBs [about 1/3 of *SWIFT* GRBs can be considered ‘dark’, e.g. Schady et al. (2007)], lacking a detection of the optical afterglow. Dark GRBs should largely comprise a population of high z events, rather than highly extinguished systems.
- The young age of hosts implies that (i) the specific SFR is high ($\dot{M}_{\star}/M_{\star} \gtrsim 2 \times 10^{-8}$) and (ii) the ratios of abundance of different chemical elements are just those of the respective chemical yields of type II SNaE, i.e. large α -enhancements should be the rule.
- Most of the hosts ($10^9 \lesssim M_{\text{H}} \lesssim 10^{11} M_{\odot}$) have UV magnitude in the range $-20 \lesssim M_{1350} \lesssim -16$ and $\text{Ly}\alpha$ luminosity in the range $2 \times 10^{40} \lesssim L_{\text{Ly}\alpha} \lesssim 2 \times 10^{42} \text{ erg s}^{-1}$. They trace the formation of small galaxies in small halos, and as a consequence the faint end of the LBG and LAE LF. These hosts would reionize the Universe at $z \approx 7$ (see Mao et al. 2007).

ACKNOWLEDGMENTS

We thank Giancarlo Ghirlanda for helpful discussions, and Gianfranco De Zotti for useful suggestions and a critical reading of the manuscript. This research is partially supported by MIUR, INAF and the NSF under Grant No. PHY99-07949. AC thanks the KITP (Santa Barbara) for kind hospitality.

REFERENCES

- Annibali, F., et al. 2007, *A&A*, 463, 455
 Band, D.L. 2006, *ApJ*, 644, 378
 Berger, E., et al. 2007, *ApJ*, 660, 504
 Bloom, J.S., et al. 2002, *AJ*, 123, 1111
 Bloom, J.S., et al. 1999, *Nature*, 401, 453
 Bouwens, R.J., et al. 2006, 653, 53
 Bromm, V., & Loeb, A. 2006, *ApJ*, 642, 382
 Bromm, V. et al. 2001, *MNRAS*, 328, 969
 Campana, S., et al. 2006, *Nature*, 442, 1008
 Castro-Tirado, A.J., & Gorosabel, J. 1999, *A&AS*, 138, 449
 Chen, H.-W., et al. 2005, *ApJ*, 634, L25
 Chabrier, G., in *The Initial Mass Function 50 Years Later*, ed. E. Corbelli and F. Palte, Dordrecht: Springer
 Christensen L., Hjorth J., Gorosabel J., 2004, *A&A*, 425, 913
 Cirasuolo, M., et al. 2005, *ApJ*, 629, 816
 Cowie, L.L., et al. 1996, *AJ*, 112, 839

- Croton, J.D., et al. 2006, MNRAS, 365, 11
- Daigne, F., Rossi, E.M., & Mochkovitch, R. 2006, MNRAS, 372, 1034
- Della Valle, M., et al. 2003, A&A, 406, L33
- Della Valle, M., et al. 2006, ApJ, 642, L103
- De Lucia, G., et al. 2006, MNRAS, 366, 499
- Djorgovski, S.G., et al. 2001, in Gamma-Ray Bursts in the Afterglow Era: 2nd Workshop, eds. E. Costa et al., Berlin: Springer Verlag, p.218
- Fiore, F., et al. 2007, A&A, 470, 515
- Firmani, C., et al. 2005, MNRAS, 360, L1
- Fruchter, A.S., et al. 2006, Nature, 441, 463
- Fruchter, A.S., et al. 1999, ApJ, 516, 683
- Fynbo, J.U., et al. 2000, ApJ, 542, L89
- Fynbo, J.U., et al. 2006, A&A, 451, L47
- Galama, T., et al. 1998, Nature, 396, 670
- Gehrels, N., et al. 2004, ApJ, 611, 1005
- Ghirlanda, G. et al. 2007, A&A, 466, 127
- Ghirlanda, G., Ghisellini, G., & Firmani, C. 2005, MNRAS, 361, L10
- Gibson, B.K., et al. 2003, PASA, 20, 401
- Glazebrook, K., et al. 2004, Nature, 430, 181
- Gorosabel, J., et al. 2005, A&A, 444, 711
- Granato, G.L., et al. 2006, MNRAS, 368, L72
- Granato, G.L., et al. 2004, ApJ, 600, 580
- Granato, G.L., et al. 2001, MNRAS, 324, 757
- Greggio, L. 2005, A&A, 441, 1055
- Guetta, D., Piran, T., & Waxman, E. 2005, ApJ, 619, 412
- Hjorth, J., et al. 2003, Nature, 423, 847
- Holland, S., & Hjorth, J., 1999, A&A, 344, L67
- Kawakatu, N., & Umemura, M. 2002, MNRAS, 329, 572
- Kodama, T., et al. 2004, MNRAS, 350, 1005
- Jakobsson, P., et al. 2005, MNRAS, 362, 245
- Langer, N., & Norman, C.A. 2006, ApJ, 638, L63
- Lapi A., et al. 2006, ApJ, 650, 42
- Le Floc'h, E., et al. 2006, ApJ, 642, 636
- Malesani, D., et al. 2004, ApJ, 609, L5
- MacFadyen, A.I., & Woosley, S.E. 1999, ApJ, 524, 262
- Mao, J., et al. 2007, ApJ, 667, 655
- Michałowski, M.J., & Hjorth, J. 2007, AIP Conf. Proc. 924, 143
- Mo, H.J., & Mao, S. 2004, MNRAS, 353, 829
- Modjaz, M., et al. 2006, ApJ, 645, L21
- Natarajan, P., et al. 2005, MNRAS, 364, L8
- Negrello, M., et al. 2007, MNRAS, 377, 1557
- Prochaska, J.X., et al. 2007, ApJ, 666, 267
- Preece, R.D., et al. 2000, ApJS, 126, 19
- Price, P.A., et al. 2007, ApJ, 663, L57
- Priddey, R.S., et al. MNRAS, 369, 1189
- Renzini, A. 2006, ARA&A, 44, 141
- Romano, D., et al. 2002, MNRAS, 334, 444
- Salvaterra, R., & Chincarini, G. 2007, ApJ, 656, L49
- Sanchez-Blazquez, P., et al. 2007, MNRAS, 377, 759
- Savaglio, S., et al. 2003, ApJ, 585, 638
- Savaglio, S., Glazebrook, K., & Le Borgne, D. 2006, in Gamma Ray Bursts in the Afterglow Era, ed. S.S. Holt, N. Gehrels, and J.A. Nousek, Melville, NY: AIP
- Schady, P., et al., 2007, MNRAS, 377, 273
- Schiminovich, D., et al. 2005, ApJ, 619, L47
- Schneider, R., et al. 2006, MNRAS, 369, 825
- Sheth, R.K., & Tormen, G. 1999, MNRAS, 308, 119
- Silva, L., et al. 2005, MNRAS, 357, 1295
- Starling, R.L.C., et al. 2005, A&A, 442, L21
- Stanek, K.Z., et al., 2003, ApJ, 591, L1
- Steidel, C.C., et al. 2001, ApJ, 546, 665
- Steidel, C. C., et al. 1999, ApJ, 519, 1
- Tanvir, N.R., & Levan, A.J., preprint 0709.0861
- Tanvir, N.R., et al., 2004, MNRAS, 352, 1073
- Tumlinson, J., et al. 2007, ApJ, 668, 667
- Wainwright, C., Berger, E., & Penprase, B.E. 2007, ApJ, 657, 367
- Woosley, S.E., 1993, ApJ, 405, 273
- Woosley, S.E., & Heger, A. 2004, in Stellar Rotation, IAU Sym. No. 215, eds. A. Maeder & Ph. Eenens
- Woosley, S.E., & Heger, A. 2006, ApJ, 637, 914
- Yoshida, M., et al. 2006, ApJ, 653, 988
- Yoon S.-C., Langer N., & Norman, C. 2006, A&A, 460, 199
- Yoon S.-C., Langer N., 2005, A&A, 443, 643
- Yoon S.-C., Langer N., 2006, in Stellar Evolution at Low Metallicity: Mass Loss, Explosions, ASP Conf. Ser. 353, p.63
- Zeh A., et al., 2004, ApJ, 609, 952
- Zhao, D.H., et al. 2003, MNRAS, 339, 12

APPENDIX A: A SIMPLE RECIPE FOR STAR FORMATION AND DUST OBSCURATION IN PROTOGALAXIES

Granato et al. (2004) have proposed a model for early galaxy formation, in which the most relevant processes (gas cooling and inflow, star formation and gas accretion onto BH, stellar and quasar feedback, gas outflow) are included in a set of equations, that can be solved with straightforward numerical computations. In this Appendix we present a simplified version of the model describing the SFR, mass in stars and chemical evolution, which are relevant for this work. The analytical formulae presented below are very good approximations of the results found by solving the full set of equations of the model (for details see Lapi et al. 2006 and Mao et al. 2007). We stress that, because of their fundamental character, the equations listed below describes the main aspects of star formation and chemical evolution in protogalaxies at high redshift.

When a DM halo of mass M_H reaches the virial equilibrium, it contains a mass $M_{\text{inf}}(0) = f_{\text{cosm}} M_H$ of hot gas at the virial temperature, $f_{\text{cosm}} \approx 0.18$ being the mean cosmic baryon to DM mass-density ratio. The gas in virial equilibrium flows toward the central region at a rate $\dot{M}_{\text{cond}} = \dot{M}_{\text{inf}}/t_{\text{cond}}$ where the *condensation* timescale $t_{\text{cond}} = \max[t_{\text{cool}}(R_H), t_{\text{dyn}}(R_H)]$, is the maximum between the dynamical time and the cooling time at the halo virial radius R_H . When computing the cooling time, a clumping factor C in the baryonic component is also included: $C \gtrsim 7$ implies $t_{\text{cool}}(R_H) \lesssim t_{\text{dyn}}(R_H)$ on relevant galaxy scales at high- z . By defining such a condensation time, we implicitly neglect the effect of angular momentum. However, angular momentum decays on a dynamical friction timescale $t_{\text{DF}} \approx 0.2 (\xi / \ln \xi) t_{\text{dyn}}$, where $\xi = M_H/M_c$ and M_c is the typical mass cloud involved in major mergers (e.g. Mo & Mao 2004); major mergers, which are very frequent at high redshift and in the central regions of halos, imply $\xi \sim$ a few.

The model also assumes that quasar activity removes the hot gas from the halo through winds at a rate $\dot{M}_{\text{inf}}^{QSO}$; the equation for the diffuse hot gas is then

$$\dot{M}_{\text{inf}} = -\dot{M}_{\text{cond}} - \dot{M}_{\text{inf}}^{QSO}. \quad (\text{A1})$$

The cold gas is piled up following the cooling of hot gas, is consumed by star formation (\dot{M}_*), and is removed by the energy feedback from SNaE ($\dot{M}_{\text{cold}}^{\text{SN}}$) and quasar activity ($\dot{M}_{\text{cold}}^{QSO}$):

$$\dot{M}_{\text{cold}} = \dot{M}_{\text{cond}} - (1 - \mathcal{R})\dot{M}_* - \dot{M}_{\text{cold}}^{\text{SN}} - \dot{M}_{\text{cold}}^{QSO}, \quad (\text{A2})$$

where \mathcal{R} is the fraction of gas restituted to the cold component by the evolved stars. Under the assumption of instantaneous recycling, $\mathcal{R} \approx 0.54$ for the adopted IMF ($\mathcal{R} \approx 0.3$ for a Salpeter IMF); this value of \mathcal{R} is an upper limit, since only a fraction of evolved stars have a significant mass loss in the evolutionary phases considered here. However, the relevant results are only very weakly sensitive to the chosen value, in the physically allowed range. The mass of

cold baryons that is going to be accreted onto the central supermassive BH is small enough to be neglected in the above equation (see Granato et al. 2004).

Stars are formed at a rate

$$\dot{M}_* = \int \frac{dM_{\text{cold}}}{\max[t_{\text{cool}}, t_{\text{dyn}}]} \approx \frac{M_{\text{cold}}}{t_*}, \quad (\text{A3})$$

where now t_{cool} and t_{dyn} refer to a mass shell dM_{cold} , and t_* is the star formation timescale averaged over the mass distribution.

The rate of cold gas removal due to SNaE is parameterized as

$$\dot{M}_{\text{cold}}^{\text{SN}} = \beta_{\text{SN}} \dot{M}_*, \quad (\text{A4})$$

where the averaged efficiency

$$\beta_{\text{SN}} = \frac{n_{\text{SN}} \epsilon_{\text{SN}} E_{\text{SN}}}{E_{\text{bind}}} \approx 0.6 \left(\frac{n_{\text{SN}}}{1.4 \times 10^{-2} / M_{\odot}} \right) \times \left(\frac{\epsilon_{\text{SN}}}{0.05} \right) \left(\frac{E_{\text{SN}}}{10^{51} \text{erg}} \right) \left(\frac{M_{\text{H}}}{10^{12} M_{\odot}} \right)^{-2/3} \left(\frac{1+z}{7} \right)^{-1} \quad (\text{A5})$$

depends on the number of SNaE per unit solar mass of condensed stars n_{SN} , the energy per SN available to remove the cold gas $\epsilon_{\text{SN}} E_{\text{SN}}$, and the specific binding energy of the gas within the DM halo, E_{bind} . Following Zhao et al. (2003) and Mo & Mao (2004), the latter quantity has been estimated, for $z \gtrsim 1$, as $E_{\text{bind}} = V_{\text{H}}^2 f(c) (1 + f_{\text{cosm}})/2 \approx 5.6 \times 10^{14} (M_{\text{H}}/10^{12} M_{\odot})^{2/3} [(1+z)/7] \text{cm}^2 \text{s}^{-2}$. Here V_{H} is the halo circular velocity at the virial radius and $f(c) \approx 2/3 + (c/21.5)^{0.7} \sim 1$ is a weak function of the halo concentration $c \sim$ a few. Lapi et al. (2006) have shown that high redshift LFs of quasars and galaxies constrain $\epsilon_{\text{SN}} \approx 0.05$; the same value is required in order to reproduce the fundamental correlations between local ellipticals and dormant BHs.

By analyzing the results of the numerical solution of the full set of equations by Granato et al. (2004), it is apparent that the term of quasar feedback is important only during the final stage of BH growth, around 2–3 e-folding times (approximately 10^8 yr) before the peak of quasar luminosity, when the energy discharged by the quasar is so powerful to unbind most of the residual gas, quenching both star formation and further accretion onto the supermassive BH. The time integral over the quasar bolometric power exceeds the gas binding energy after

$$\Delta t_{\text{burst}} \approx 2.5 \times 10^8 \left(\frac{1+z}{7} \right)^{-1.5} \mathcal{F} \left(\frac{M_{\text{H}}}{10^{12} M_{\odot}} \right) \text{yr}, \quad (\text{A6})$$

where $\mathcal{F}(x) = 1$ for $x \gtrsim 1$ and $\mathcal{F}(x) = x^{-1}$ for $x \lesssim 1$. Therefore a good approximation for the star formation history is obtained by neglecting the quasar feedback effect in Eqs. (A1) and (A2) and by abruptly stopping star formation and accretion onto the central BH after Δt_{burst} since halo virialization.

Then Eqs. (A1) and (A2) can be easily solved, with the outcome that the infalling mass declines exponentially as $M_{\text{inf}}(t) = M_{\text{inf}}(0) e^{-t/t_{\text{cond}}}$, while the SFR evolves according to

$$\dot{M}_*(t) = \frac{M_{\text{inf}}(0)}{t_{\text{cond}}(\gamma - 1/s)} \left[e^{-t/t_{\text{cond}}} - e^{-s\gamma t/t_{\text{cond}}} \right], \quad (\text{A7})$$

with $\gamma \equiv 1 - \mathcal{R} + \beta_{\text{SN}}$. The quantity $s \equiv t_{\text{cond}}/t_*$ is the ratio between the timescale for the large-scale infall estimated at the virial radius and the star formation timescale in the central region; it corresponds to $s \sim 5$, both for an isothermal or NFW (Navarro et al. 1997) density profile.

The following expression well approximates the condensation timescale (see Mao et al. 2007):

$$t_{\text{cond}} \approx 4 \times 10^8 \left(\frac{1+z}{7} \right)^{-1.5} \left(\frac{M_{\text{H}}}{10^{12} M_{\odot}} \right)^{0.2} \text{yr}. \quad (\text{A8})$$

The scaling with redshift reflects the dependence of the dynamical time; the weak dependence on M_{H} reproduces the impact of the energy feedback from the quasar on the infalling gas, which is stronger for more massive halos hosting more massive BH.

In order to compute the metal content of the cold gas, one has to take into account the infall of primordial abundance gas, the enrichment due to earlier generations of stars, and outflows driven by winds generated by SNaE and quasars. We assume, as common, that in the cold gas there is an instantaneous mixing of metals released by stars. The corresponding simplified equation reads

$$\dot{Z}_{\text{cold}}(t) = \frac{Z_{\text{inf}} - Z_{\text{cold}}}{t_{\text{cond}}} \frac{M_{\text{inf}}(t)}{M_{\text{cold}}(t)} + \frac{\mathcal{R}_Z(t)}{t_*}, \quad (\text{A9})$$

where

$$\mathcal{R}_Z(t) \approx \int_{m_{*,t}}^{m_{*,\text{sup}}} dm_* m_* q_Z(m_*) \phi(m_*) \frac{\dot{M}_*(t - \tau_{m_*})}{M_*(t)}. \quad (\text{A10})$$

The IMF is denoted by $\phi(m_*)$ and $q_Z(m_*)$ is the metal yield of stars of mass m_* . From Fig. 1 it is apparent that metallicity rapidly (in a time less than a few 10^8 Gyr) increases from primordial content to the limiting value

$$Z_{\text{cold}} \approx \frac{s}{s\gamma - 1} A_Z, \quad (\text{A11})$$

with $A_Z = 0.043$ for the adopted IMF ($A_Z = 0.021$ for the Salpeter IMF).

In early galaxy evolution an important role is played by dust, that absorbs the UV emission and re-radiates it in the mid and far-IR band. The amount of dust in a galaxy is expected to be correlated with that of cold gas [or SFR, see Eq. (A3)] and with metallicity. Mao et al. (2007) have shown that it is possible to describe the luminosity-reddening relation found by Shapley et al. (2001) for $z \approx 3$ LBGs with the simple law

$$A_{1350} \approx 0.35 \left(\frac{\dot{M}_*}{M_{\odot} \text{yr}^{-1}} \right)^{0.45} \left(\frac{Z}{Z_{\odot}} \right)^{0.8}, \quad (\text{A12})$$

where A_{1350} is the attenuation at 1350 Å. By inserting in the above equation the SFR and metallicity, we get the attenuation as function of time. Then the UV magnitude is simply given by

$$M_{1350} \approx -18.6 - 2.5 \log \left(\frac{\dot{M}_*}{M_{\odot} \text{yr}^{-1}} \right) + A_{1350}. \quad (\text{A13})$$

This simplified treatment of dust attenuation proved to be quite a good approximation for low-luminosity LBGs and LAEs, which exhibit low attenuation (Mao et al. 2007).

On the other hand, for massive halos attenuation is large soon after 10^8 yr; this corresponds to the quick appearance of very luminous submm-selected galaxies. For these systems the model by Granato et al. (2004) includes a sophisticated treatment of dust attenuation through the GRASIL code (Silva et al. 1998).

The scheme presented here traces the evolution of single galaxy halos as function of time, given their mass and their formation redshift. The results can be interfaced to the formation rate, $d^2 N_{\text{ST}}/dM_{\text{H}} dt_z$ (see § 2.2) yielding LFs, counts and redshift distribution for spheroidal galaxies. Moreover, the quasar LF can also be reproduced (Lapi et al. 2006), as well as the LF of LBGs and Ly α emitters (Mao et al. 2007). A summary of the parameters used by the model and of its achievements is presented in Tables 1 and 2 of Lapi et al. (2006).